

Extended star-forming region within galaxies in a dense proto-cluster core at $z=2.53$ *

Tomoko L. Suzuki^{1,2}, Yosuke Minowa^{3,4}, Yusei Koyama^{3,4}, Tadayuki Kodama¹, Masao Hayashi², Rhythm Shimakawa³, Ichi Tanaka³, Ken-ichi Tadaki²

Abstract

At $z \sim 2$, star-formation activity is thought to be high even in high-density environments such as galaxy clusters and proto-clusters. One of the critical but outstanding issues is if structural growth of star-forming galaxies can differ depending on their surrounding environments. In order to investigate how galaxies grow their structures and what physical processes are involved in the evolution of galaxies, one requires spatially resolved images of not only stellar components but also star-forming regions within galaxies. We conducted the Adaptive Optics(AO)-assisted imaging observations for star-forming galaxies in a dense proto-cluster core at $z = 2.53$ with IRCS and AO188 mounted on the Subaru Telescope. A combination of AO and narrow-band filters allows us to obtain resolved maps of $H\alpha$ -emitting regions with an angular resolution of 0.1–0.2 arcsec, which corresponds to ~ 1 kpc at $z \sim 2.5$. Based on stacking analyses, we compare radial profiles of star-forming regions and stellar components and find that the star-forming region of a sub-sample with $\log(M_*/M_\odot) \sim 10 - 11$ is more extended than the stellar component, indicating the inside-out growth of the structure. This trend is similar to the one for star-forming galaxies in general fields at $z = 2 - 2.5$ obtained with the same observational technique. Our results suggest that the structural evolution of star-forming galaxies at $z = 2 - 2.5$ is mainly driven by internal secular processes irrespective of surrounding environments.

Fig 1. Sample

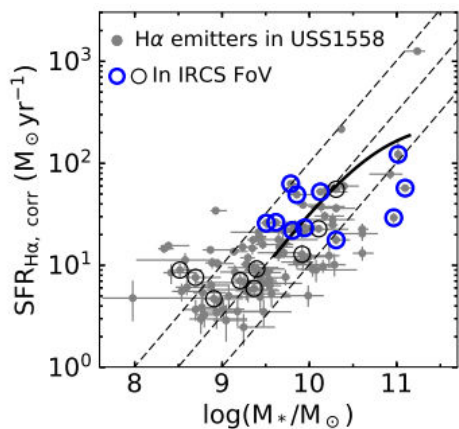


Fig. 1. Stellar mass–SFR relation for the $H\alpha$ emitters in USS1558 (Hayashi et al. 2012, 2016; Shimakawa et al. 2018). Open circles show the $H\alpha$ emitters covered in the IRCS FoV. The blue thick ones correspond to the $H\alpha$ emitters analyzed in this study (subsection 2.2). Dotted lines represent constant sSFRs (SFR/M_*), namely, $\log(sSFR [\text{yr}^{-1}]) = -8.0, -8.5, \text{ and } -9.0$. The thick solid line shows the star-forming main sequence at $z = 2.53$ from Tomczak et al. (2016). Our IRCS+AO188 targets are located around the “main sequence” of star-forming galaxies at this epoch.

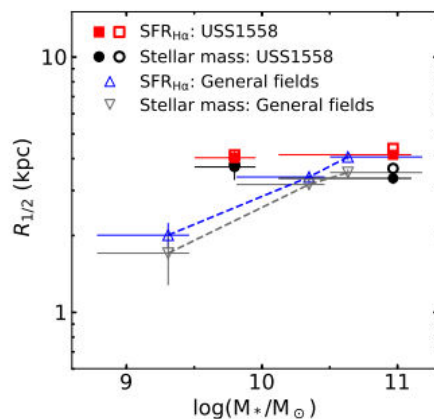


Fig. 6. Relation between the total stellar mass and size of the stellar components and star-forming regions for the $H\alpha$ emitters in different density fields at $z \sim 2 - 2.5$. The sizes measured in the stacked images are shown for the two samples. The filled symbols represent $R_{1/2}$ assuming the radially dependent $A_{H\alpha}$, whereas the open symbols represent $R_{1/2}$ obtained with the uniform $A_{H\alpha}$. Both in the general fields and in the proto-cluster core, star-forming regions are more extended than the underlying stellar components at least for the massive star-forming galaxies with $\log(M_*/M_\odot) \sim 10 - 11$.

$z \sim 2.5$ proto-cluster 銀河の構造形成過程

arXiv.1904.00695

- $z \sim 2.5$ proto-clusterの中心部のAO+NB撮像
- Low mass, high massに分けてそれぞれでstacking
- Stellar componentとstar-forming regionのradial profileを比較。
 - 進化過程 (compaction or secular) を考察。

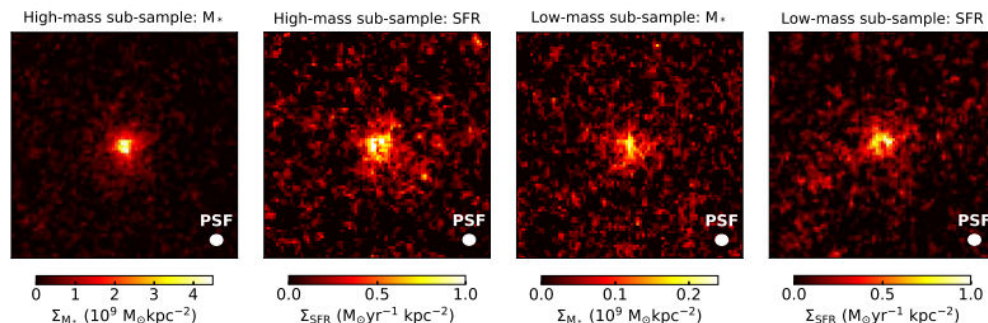


Fig. 4. Stacked images of the stellar mass and $SFR_{H\alpha, \text{corr}}$ for the two sub-samples with the radially dependent $A_{H\alpha}$ (subsection 4.1). The box size of each panel is $\sim 4.3 \times 4.3$ arcsec². The small white circle in each panel shows the PSF size (FWHM).

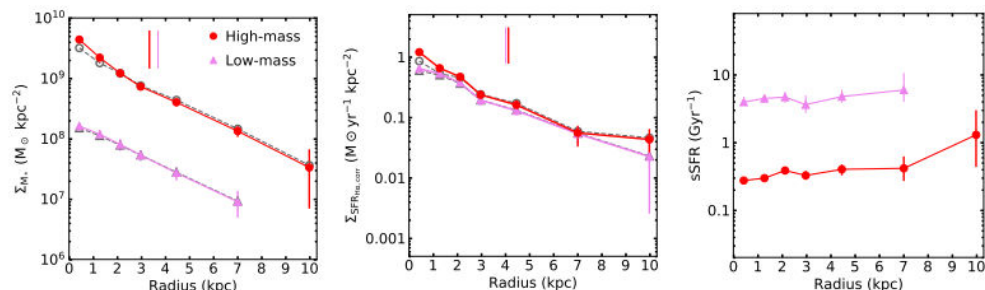


Fig. 5. Radial profiles of the two sub-samples. From the left to right, each panel shows the radial profiles of stellar mass surface density, those of SFR surface density, and those of sSFR. In the left and the middle panels, the filled symbols represent the results using the radially dependent $A_{H\alpha}$ (subsection 4.1). The open symbols represent the results with the uniform $A_{H\alpha}$. The vertical lines in the left and middle panel represent $R_{1/2}$ for the stellar component and star-forming region with the radially dependent $A_{H\alpha}$. The thick ones show $R_{1/2}$ for the high-mass sub-sample. The SFR profiles of the two sub-samples have a flatter slope than the stellar mass profiles.

Fig 5. stellar mass, SFRのradial profile

- High mass: 星形成領域が星質量に比べて広がっている。
- Low mass: disk全面で活発。

Fig 6. Field 銀河との比較

- High mass側では、環境に寄らず $R(SF) > R(star) \rightarrow$ inside-out.
- Low mass側では、cluster環境の方がサイズが大きい sample bias (high sSFR) の影響もある。

- 現在のSFR (radial profile) が続くと仮定すると、high mass, low massどちらのサンプルも(gas-rich merger等ではなく) secularにinside-out的にmass assemblyすると予想される。
- この時代の星形成銀河は環境に寄らずsecularに生長しているようだ。